# An automatic initialization procedure in parameter estimation problems with parameter-affine dynamic models.

J. Bonilla[a,b], M. Diehl[b], F. Logist[a], B. De Moor[b], J. Van Impe[*,a]

[a] *Department of Chemical Engineering CIT/BioTeC, Katholieke Universiteit Leuven, W. De Croylaan 46, B-3001 Leuven, Belgium.*
[b] *Department of Electrical Engineering ESAT/SCD, Katholieke Universiteit Leuven, Kasteelpark Arenberg 10, bus 2446 B-3001 Leuven, Belgium.*

**Abstract**

This paper proposes an initialization approach for parameter estimation problems (PEPs) involving parameter-affine dynamic models. By using the state measurements, the nonconvex PEP is modified such that a convex approximation to the original PEP is obtained. The modified problem is solved by convex optimization methods yielding an approximate solution to the original PEP. The approximate solution can be further refined by linearizing the original problem around the obtained minimum. An assessment of the distance between the real solution and the one provided by the linearization of the problem around the convex approximation is presented. The optimum obtained by the convex approximation is used to subsequently initialize a Simultaneous Gauss-Newton (SGN) approach on the original nonconvex PEP. Comparative results for the SGN with arbitrary initialization and with the proposed approach are presented using three benchmark examples in the chemical and biological fields.

*Key words:* Parameter estimation, Multiple shooting, convex optimization.

[*]Corresponding author. Tel: +32 16 321466; fax: +32 16 32299.
*Email address:* jan.vanimpe@cit.kuleuven.be (J. Van Impe)

## 1. Introduction

Developing accurate models for dynamic processes has an enormous impact on science and engineering. Models used to predict and control process dynamics are basically characterized by their structure and the parameter values in this structure. Parameter estimation addresses the calculation of a set of parameter values in a predefined model structure, such that the outputs of the model fit the measurement data. Approaches to fit the collected data to a given model generally lie in one of the following classes: *(i)* the ones which minimize the errors between data and model outputs with respect to a given norm and *(ii)* the ones which demand errors to be uncorrelated with the measured data sequence (Ljung, 1999). Fitting is not the only requirement in the parameter estimation problem (PEP), constraints on the estimated parameter and model states are usually required as well, e.g., positive reaction rates, upper and lower bounds in concentrations. Consequently, PEPs are often cast as optimization problems, leading to convex or nonconvex formulations depending on the nature of the fitting criteria, the model and the constraints. Nonlinear models generally lead to nonconvex PEPs which are difficult to solve since they can exhibit local solutions and the true parameter can be hard to find.

In order to tackle PEPs involving dynamic models, several methods have been proposed. On the one hand, the methods based on calculus of variations and Pontryagin's maximum principle (Pontryagin, 1962) are known as *indirect methods* and, on the other hand, the methods based on the finite parameterization of the continuous functions involved in the optimization task are called *direct methods*. It has to be mentioned that the latter methods are preferred when the optimization problem possesses inequality constraints since the former methods become difficult to solve under this condition unless information regarding the active constraints is available (Cervantes and Biegler, 1999). Among the direct methods, the most reliable approaches for PEP are based on *Simultaneous Optimization* (Biegler et al., 2002) combined with constrained Gauss-Newton method (Nocedal and Wright, 2006), or constrained $L_1$ estimation method (Kostina, 2004). Two of the most widely used simultaneous optimization techniques are *direct multiple shooting* (Bock and Plitt, 1984) and *collocation on finite elements* (Biegler, 1984). Despite of the efficiency and robustness of these methods, they still require a starting point to initialize the optimization routines. The current work proposes an initialization method for nonconvex PEPs involving a particular class of dynamic

models, namely parameter-affine systems. The proposed approach leads to a convex problem, where initialization is not required, and a solution can easily be obtained by convex optimization tools (Boyd and Vandenberghe, 2006). Hereafter, the solution of this convex problem can be used to initialize the nonconvex PEP combined with a simultaneous optimization technique.

Other well-known procedures leading to convex problems have been proposed for parameter-affine systems, such as Least Squares Prediction Error Methods LS-PEM (Ljung, 2002). Although these methods are widely used, they are sensitive to noisy data and in order to work well in practice, they need to filter the residuals. On the contrary, the approach presented here does not involve the use of arbitrary filters over the residuals and can be shown to be less sensitivity to noisy data, leading to less biased results without previous knowledge of the errors' behavior (Bonilla et al., 2008).

*Main contribution of the paper*

The main contribution of this work is the proposed initilization method for parameters estimation problems involving parameter affine dynamic models. Moreover, the initialization procedure is analyzed and an assesment of the distance betweeen the initial guess proposed by the approach and the minimum of the nonconvex problem is provided. In adition, the use of the method combined with efficient simultanoeus optimization techniques is illustrated through benchmark examples, showing the advantages of using the approach against an arbitrary initialization.

The paper is organized as follows: Section 2 introduces the Least Squares Parameter Estimation Problem (LS-PEP) for nonlinear systems. Section 3 presents the proposed approach for parameter estimation using a least squares norm and a parameter-affine model. Section 4 introduces the principles of simultaneous optimization in the multiple shooting framework employing the constrained Gauss-Newton method. Numerical examples comparing the known approaches with the proposed method are presented in Section 5. Conclusions follow in Section 6.

## 2. Parameter Estimation for Dynamic Processes

Consider the dynamics of a process during a given time interval $[0, T]$, modeled by an Ordinary Differential Equation (ODE) of the form:

$$\dot{x}(t) = \Phi(x(t), p), \quad t \in [0, T], \tag{1}$$

where the vector $p \in \mathbb{R}^{n_p}$ and $x(t) \in \mathbb{R}^{n_x}$ denote model parameters and states, respectively. In order to estimate the value of the vector $p$, a set of measurements $y(t_i) \in \mathbb{R}^{n_y}$, $i = 0, 1, \ldots, n_m$ with $n_m + 1 \geq n_p$, is collected along the interval of interest. The set of measurements $y(t_i)$ does not necessarily correspond to the model states at the sampling points $x(t_i)$, however, here it is assumed that the measurement set corresponds to measurements of the system states, i.e., $y(t_i) = \bar{x}(t_i)$. The mismatch between the output of the model (1) and the measurements are usually quantified using a Least Squares (LS) norm:

$$\mathcal{J}(x(t_i), \bar{x}(t_i)) = \frac{1}{2} \sum_{i=0}^{n_m} \sum_{j=1}^{n_x} (x_j(t_i) - \bar{x}_j(t_i))^2. \tag{2}$$

Although $L_1$-cost minimization may be less sensitive to the presence of outliers in the measurement set[1], the $L_2$-norm is widely applied due to its smoothness and is considered in the current study. Following the introduced notation, the PEP can be cast in the form:

$$\min_{p, x(.)} \mathcal{J}(x(t_i), \bar{x}(t_i)), \tag{3}$$

subject to:

$$\begin{aligned} \dot{x}(t) &= \Phi(x(t), p), \quad t \in [0, T], & (4)\\ x(t) &\in \mathbb{X}, \quad t \in [0, T], & (5)\\ p &\in \mathbb{P}. & (6) \end{aligned}$$

Constraints on the parameters and model states can be introduced by the sets $\mathbb{P}$ and $\mathbb{X}$ respectively. Consequently, parameter estimation tasks are considered as optimization problems and may lead to nonconvex formulations, particularly when $\Phi(x(t), p)$ is nonlinear in the states.

In the following, a particular structure in the general NLS-PEP (3)-(6) is considered. It is assumed that the nonlinear model exhibits a parameter-affine form:

$$\Phi(x(t), p) = \Gamma(x(t)) + \Upsilon(x(t))p, \tag{7}$$

and the set described by $\mathbb{X} \times \mathbb{P}$ is convex. Bound constraints on parameters and states are the simplest case covered by the assumption on the convexity of the set $\mathbb{X} \times \mathbb{P}$.

[1] $L_1$ norm does not square the contribution of the errors.

## 3. The Convex Approach

The approach proposed is inspired by continuation methods in optimization (Watson, 2000). These kind of methods attempt to solve an optimization problem by first solving a related optimization task which is hopefully connected to the original one by a continuous path. The nonconvex PEP (3)-(6) can be reformulated using this approach by introducing a homotopy parameter $\lambda \in (0, 1)$, a new variable $\tilde{x}(t)$ and a norm on this new variable in the cost:

$$P(\lambda): \min_{\tilde{x}(.),x(.),p} \frac{1}{\lambda}\mathcal{J}(x(t_i), \bar{x}(t_i)) + \frac{1}{1-\lambda}\mathcal{J}(\tilde{x}(t_i), x(t_i)), \tag{8}$$

subject to

$$\begin{aligned} \dot{\tilde{x}}(t) &= \Gamma(x(t)) + \Upsilon(x(t))p, \quad t \in [0,\, T], && (9)\\ \tilde{x}(t) &\in \mathbb{X}, \quad t \in [0,\, T], && (10)\\ p &\in \mathbb{P}. && (11) \end{aligned}$$

Although the addition of the norm $\mathcal{J}(\tilde{x}(t_i), x(t_i))$ may look arbitrary, $\tilde{x}(t_i) - x(t_i)$ corresponds to the integral of the modeling errors. The parametric optimization problem (8)-(11) exhibits an interesting behavior when $\lambda$ ranges from zero to one. Although the convergence of the parametric problem solution to the global solution of the original PEP is only guaranteed if the algorithm is able to find the global solution for each $P(\lambda),\ \lambda \in (0,\ 1)$ (Bonilla et al., 2009), the approach proposed here does not attempt to follow a path for different values of $\lambda$. Consequently, the approach does not deal with methods to follow such a path of minimizers neither on the existence or continuity of that path. Moreover, the condition of a global solution is only easily satisfied for the first problem on the homotopy path namely $P(0)$ where a convex problem is addressed (Bonilla et al., 2008). It can be shown that when $\lambda$ goes to one, the problem recovers its original form, i.e., $\mathcal{J}(\tilde{x}(t_i), x(t_i))$ goes to zero, leading to (3)-(6). On the other hand, when $\lambda$ goes to zero the model states approach the measurements, i.e. $x(t_i)$ goes to $\bar{x}(t_i)$. The formulation (8)-(11) resembles quadratic penalty methods for constrained optimization (Gould, 1989) and its convergence properties can be analyzed by using the same principles (Nocedal and Wright, 2006). In the following, the problem corresponding to the case $\lambda$ going to zero:

$$P(0) : \min_{p,\tilde{x}(.)} \mathcal{J}(\tilde{x}(t_i), \bar{x}(t_i)), \tag{12}$$

subject to

$$\begin{aligned} \dot{\tilde{x}}(t) &= \Gamma(\bar{x}(t)) + \Upsilon(\bar{x}(t))p, \quad t \in [0, T], && (13)\\ \tilde{x}(t) &\in \mathbb{X}, \quad t \in [0, T], && (14)\\ p &\in \mathbb{P}, && (15) \end{aligned}$$

is used as a convex modification of the original nonconvex PEP. Notice that only the convex extreme of the homotopy map is considered. In fact, the homotopy map is mentioned here only to show that there is a link between the original problem and the convex modification. Convexity is achieved in this formulation since $(i)$ the cost is quadratic in the pseudo-states $\tilde{x}(t)$, $(ii)$ the nonlinearity in the model has vanished by introducing the measurement trajectories $\bar{x}(t)$, $(iii)$ the model is affine in the parameters $p$ and $(iv)$ the feasible set $\mathbb{X} \times \mathbb{P}$ is convex. Although the modification in the model could be seen as a linearization around measurements, it differs from that approach since no information of a linearization point for the parameters, $\bar{p}$, is provided. Figure 1 illustrates the homotopy map generated by the parametric optimization problem (8)-(11) when applied to the estimation of the natural frequency $\omega_n$, in a harmonic oscillator model (Bonilla et al., 2007). Notice that, as mentioned previously, the extreme of the map corresponding to $P(0)$ is convex.

It is possible to refine the solution provided by the convex approach by further linearizing the original problem around the solution to $P(0)$. This refinement corresponds to the first iteration in a *Sequential Quadratic Programming* (SQP) method when the initial guess is set to the solution provided by $P(0)$. In the following, it is proven that this refinement delivers a solution with a distance from the real optimum of second order in the size of problem perturbations[2]. This is clarified in the following section.

### *3.1. Assessment of the approximation errors*

In this section, an assessment of the distance between the real solution to the PEP and the solution provided by the refined convex problem is ana-

[2]By problem perturbations we mean measurement noise and modeling errors.

lyzed. In order to do so, the optimization problems (3)-(6) and (12)-(15) are parameterized using a suitable discretization method, leading to:

$$\text{PEP}_{\text{NL}}(\bar{\mathbf{x}}): \quad \min_{p,\mathbf{x}} \frac{1}{2} \parallel \mathbf{x} - \bar{\mathbf{x}} \parallel_Q^2, \tag{16}$$

subject to

$$\begin{aligned} \mathbf{0} &= A(\mathbf{x}) - B(\mathbf{x})p - W\mathbf{x}, & (17)\\ \mathbf{x} &\in \mathbb{X}, \quad p \in \mathbb{P}, & (18) \end{aligned}$$

and

$$\text{PEP}_{\text{CVX}}(\bar{\mathbf{x}}): \quad \min_{p,\tilde{\mathbf{x}}} \frac{1}{2} \parallel \tilde{\mathbf{x}} - \bar{\mathbf{x}} \parallel_Q^2, \tag{19}$$

subject to

$$\begin{aligned} \mathbf{0} &= A(\bar{\mathbf{x}}) - B(\bar{\mathbf{x}})p - W\tilde{\mathbf{x}}, & (20)\\ \tilde{\mathbf{x}} &\in \mathbb{X}, \quad p \in \mathbb{P}, & (21) \end{aligned}$$

where $\mathbf{x} = [x(t_0)^T, x(t_1)^T, \ldots, x(t_N)^T]^T$ and $\bar{\mathbf{x}} = [\bar{x}(t_0)^T, \bar{x}(t_1)^T, \ldots, \bar{x}(t_N)^T]^T$ correspond to the discrete time model state dynamics and the state measurements, respectively. $A(\mathbf{x})$, $B(\mathbf{x})$ and $W$ represent the nonlinear dynamics of the model along with the discretization method. $Q$ is a positive definite penalization matrix of the appropriate dimensions.

The first SQP iteration in a nonlinear programing solver linearizes the original nonconvex problem around the initial guess and solves a problem of the form

$$\text{PEP}_{\text{CVX-REF}}(\bar{\mathbf{x}}): \quad \min_{p,\mathbf{x}} \frac{1}{2} \parallel \mathbf{x} - \bar{\mathbf{x}} \parallel_2^2, \tag{22}$$

subject to

$$\begin{aligned} 0 &= A_{\text{L}}\mathbf{x} - B_{\text{L}}p + b, & (23)\\ \mathbf{x} &\in \mathbb{X}, \quad p \in \mathbb{P}. & (24) \end{aligned}$$

where (23) corresponds to the model linearized around the solution of the convex problem $(\mathbf{x}^*_{\text{CVX}}, p^*_{\text{CVX}})$. For comparison, consider the unperturbed original PEP where a set of noise-free state measurements $\bar{\bar{\mathbf{x}}}$ is obtained and no modeling errors are present. In addition, the following assumptions are introduced:

- A1: The functions $A(\mathbf{x})$ and $B(\mathbf{x})$ are twice continuously differentiable.
- A2: There exist a pair $\bar{\bar{\mathbf{x}}} \in \mathbb{X}$ and $\bar{\bar{p}} \in \mathbb{P}$ such that $0 = A(\bar{\bar{\mathbf{x}}}) - B(\bar{\bar{\mathbf{x}}})\bar{\bar{p}} - W\bar{\bar{\mathbf{x}}}$.
- A3: Both problems, $\mathrm{PEP}_{\mathrm{NL}}(\bar{\bar{\mathbf{x}}})$ and $\mathrm{PEP}_{\mathrm{CVX}}(\bar{\bar{\mathbf{x}}})$, satisfy the strong second order sufficient conditions (SOSC), strict complementarity and constraint regularity (Nocedal and Wright, 2006) at their solution, $(\bar{\bar{\mathbf{x}}}, \bar{\bar{p}})$.

**Corollary 1.** *Under assumptions A2 and A3, the Lagrange multipliers associated to the inequality constraints at the solution $(\bar{\bar{\mathbf{x}}}, \bar{\bar{p}})$ are zero, and none of the inequality constraints is active.*

In view of these assumptions, the following lemmata can be formulated:

**Lemma 1.** *If assumptions A2 and A3 hold, then $(\bar{\bar{\mathbf{x}}}, \bar{\bar{p}})$ is a global solution to all problems $\mathrm{PEP}_{\mathrm{NL}}(\bar{\bar{\mathbf{x}}})$, $\mathrm{PEP}_{\mathrm{CVX}}(\bar{\bar{\mathbf{x}}})$ $\mathrm{PEP}_{\mathrm{CVX-REF}}(\bar{\bar{\mathbf{x}}})$.*

Proof. $(\bar{\bar{\mathbf{x}}}, \bar{\bar{p}})$ is feasible and it yields the lowest possible objective value for all optimization problems, i.e., zero.

Lemma 1 states that the convex approximation provides an exact solution if the measured trajectory can be exactly generated by the model to fit, i.e., $\bar{\mathbf{x}}$ is noise-free and there are no modeling errors.

**Lemma 2.** *If A1 to A3 hold, then*

$$\|p^*_{\mathrm{cvx}}(\bar{\mathbf{x}}) - \bar{\bar{p}}\| = \mathcal{O}(\|\bar{\mathbf{x}} - \bar{\bar{\mathbf{x}}}\|), \tag{25}$$

*i.e., the distance between the perturbed convex problem solution and the unperturbed one is a function of the size of the perturbation.*

The proof to Lemma 2 is provided in the appendix.

**Theorem 1.** *If Assumptions A1 to A3 are satisfied, then*

$$\|p^*(\bar{\mathbf{x}}) - p^*_{\mathrm{CVX-REF}}(\bar{\mathbf{x}})\| = \mathcal{O}(\|\bar{\mathbf{x}} - \bar{\bar{\mathbf{x}}}\|^2) \tag{26}$$

*holds. Equation (26) gives an assessment of the distance between the original problem solution and the solution provided by the refined convex approach $p^*_{\mathrm{CVX-REF}}(\bar{\mathbf{x}})$ as a function of the size of the perturbation $\|\bar{\mathbf{x}} - \bar{\bar{\mathbf{x}}}\|$.*

The proof of Theorem 1 is provided in the appendix. This theorem is numerically corroborated by performing six experiments over a harmonic oscillator model (Bonilla et al., 2009). In each one of these experiments, a state sequence, contaminated with Gaussian noise with different variances, is collected. The distance between the solution to the PEP (3)-(6), provided by a nonlinear optimizer, and the solution proposed by the linearization of the original problem around $p^*_{\mathrm{CVX}}$ is calculated along with the size of the perturbation with respect to the noise-free data. Figure 2 (bottom) illustrates that the distance between the actual solution $p^*(\bar{\mathbf{x}})$ an the one provided in the first SQP iteration $p^*_{\mathrm{CVX-REF}}(\bar{\mathbf{x}})$ is of second order in the size of the perturbation. Notice that a second order polynomial accurately fits the data corresponding to the six experiments.

In the following, the presented convex approximation is combined with a simultaneous optimization algorithm in order to provide an initialization-free estimation methodology for parameter-affine models.

## 4. Simultaneous Optimization for PEP

The parameter estimation problem is solved here using direct approaches. There are several techniques to deal with this kind of problems, e.g., direct single shooting, multiple shooting and collocation. In single shooting the initial value problem (IVP) given by the ODE model is solved such that the states trajectories are eliminated from the optimization problem and the optimization is performed only in terms of the parameters to be estimated and the states initial condition, $x(0)$. Single shooting has been widely used, however, other direct methods have been proven to be more efficient when dealing with highly nonlinear and/or unstable process. In this work, the PEP is discretized using a direct multiple shooting (DMS) approach (Bock and Plitt, 1984). Nevertheless, other direct techniques such as collocation on finite elements (Biegler, 1984) are widely applied as well. In the following the main principles of the employed method are described.

### *4.1. The Direct Multiple Shooting Parameterization*

In DMS the measurement horizon $T$ is divided in $N$ subintervals:

$$t_0 < t_1 < t_2 \ \ldots \ < t_N = T. \tag{27}$$

The process states are parameterized on each subinterval, $N_i = [t_i,\, t_{i+1}]$, $i = 0, \ldots, N-1$, i.e., state trajectories are determined by the state values at

shooting nodes $\mathbf{s} = [s_0, s_1 \dots s_N]$, the model equations and local parameters $\mathbf{p} = [p_0, p_1 \dots p_{N-1}]$. This parameterization allows the model to be independently integrated from $t_i$ to $t_{i+1}$, $i = 0, \dots, N-1$. Figure 3 illustrates the approach followed by DMS.

Contrary to single shooting, in DMS the states are not directly eliminated from the optimization but the algorithm optimizes in initial conditions at each shooting node $s_i$ and parameters $p_i$ in each shooting interval. Note that the parameter vector $p$ is a global variable, i.e., it does not change from one shooting interval to the other, however, to make each subinterval totally independent, local variables $p_i$ can be introduced[3]. In order to guarantee continuity in the solution from $t_0$ to $t_N$ and to avoid time varying parameters, additional equality constraints are imposed on each subinterval $N_i$, i.e., the final states value of the subinterval $N_i$ must match the initial states value of the interval $N_{i+1}$, and $p_i = p_0$ for all $i = 1, 2, \dots, N-1$.

Following the DMS parameterization, the least squares PEP is reformulated as:

$$\min_{\mathbf{s},\mathbf{p}} f(\mathbf{s}, \mathbf{p}) = \frac{1}{2} \sum_{i=0}^{N} r_i^2(s_i, p_i) \tag{28}$$

subject to

$$\begin{aligned} 0 &= s_{i+1} - x(t_{i+1}), \quad i \in [0,\ N-1], && (29)\\ 0 &= p_i - p_0, \quad i \in [1,\ N-1], && (30)\\ 0 &\leq H(s_i, p_i), \quad i \in [0,\ N], && (31) \end{aligned}$$

with

$$x(t_{i+1}) = \int_{t_i}^{t_{i+1}} \Phi(s_i, p_i, t) dt + s_i.$$

The function $H(s_i, p_i)$ represents the inequality constraints imposed to the parameters and states at each shooting node. For parameter estimation,

[3]This procedure yields sparse banded Jacobian matrices

the cost to be minimized presents a pointwise feature, i.e., the cost is given by the evaluation of the residuals at the measurement instants which coincides with the selected grid for the DMS parameterization. Consequently, the parameterized problem has the general form:

$$\min_{\mathbf{w}} \frac{1}{2} \sum_{i=0}^{N} r_i^2(w_i), \tag{32}$$

subject to

$$\begin{aligned} G(\mathbf{w}) &= 0, & (33)\\ H(\mathbf{w}) &\geq 0. & (34) \end{aligned}$$

with

$$\begin{aligned} \mathbf{w} &= [w_0,\ w_1, \ldots, w_N],\\ w_i &= [s_i, p_i]\ \forall\ i = 0, 1, \ldots, N. \end{aligned}$$

Notice that for notational purposes an additional variable $p_N$ has been added since $w_N = s_N$. The presented nonlinear constrained least squares problem is usually solved using SQP algorithms. Moreover, due to the parameterization, the sub-Quadratic Programming (QP) problems arising at each SQP iterations exhibit banded and sparse structures. This sparsity and special structure can be efficiently exploited by the QP algorithm.

*4.2. The Gauss-Newton Method for PEP*

Due to the least squares form of the objective function in (32), a modified Newton's method can be used to generate the second-order information on the cost required by the SQP approach. Classical SQP methods require the Hessian of the Lagrangian, usually approximated from first-order information by update formulas such as BFGS[4]. The point-wise cost

$$f(\mathbf{w}) = \frac{1}{2} \sum_{i=0}^{N} r_i^2(w_i) = \frac{1}{2} \|R(\mathbf{w})\|_2^2, \tag{35}$$

[4]In simultaneous optimization this update is performed by blocks in order to preserve the sparsity of the Hessian.

can be formulated in terms of the residual vector

$$R(\mathbf{w}) = [r_0(w_0),\ r_1(w_1),\ \ldots, r_N(w_N)]^T\,. \tag{36}$$

By defining the Jacobian of the residual vector as:

$$J_r(\mathbf{w}) = \frac{\partial R(\mathbf{w})}{\partial \mathbf{w}} = \nabla R(\mathbf{w})^T, \tag{37}$$

the gradient and Hessian of the cost can be expressed by:

$$\nabla f(\mathbf{w}) = J_r(\mathbf{w})^T R(\mathbf{w}), \tag{38}$$

$$\nabla^2 f(\mathbf{w}) = J_r(\mathbf{w})^T J_r(\mathbf{w}) + \sum_{i=0}^{N} r_i(w_i)\nabla^2 r_i(w_i), \tag{39}$$

respectively. Note that due to the multiple shooting parameterization, the Jacobian of the residuals is sparse and banded. Normally, the second term in the right hand side of (39) is neglected since close to the solution either the residuals $r_i(w_i)$ or $\nabla^2 r_i(w_i)$ are small (Nocedal and Wright, 2006). Notice also that contrary to single shooting, in DMS, the shooting nodes are initialized with the available measurements, leading to a small residual vector at the first SQP iteration agreeing with approximation in the Gauss-Newton method and improving the convergence of the method. The proposed initialization approach complements this set of available state measurements by providing an initial guess to the parameters and avoiding an arbitrary initialization. The approximation of the Hessian of the cost leads to the main feature of Gauss-Newton method where at each mayor iteration, $k$, of the SQP a subproblem of the form

$$\min_{\Delta \mathbf{w}_k} \frac{1}{2} \| R(\mathbf{w}_k) + \nabla R(\mathbf{w}_k)^T \Delta \mathbf{w}_k \|_2^2, \tag{40}$$

subject to

$$\begin{aligned} G(\mathbf{w}_k) + \nabla G(\mathbf{w}_k)^T \Delta \mathbf{w}_k &= 0, & (41)\\ H(\mathbf{w}_k) + \nabla H(\mathbf{w}_k)^T \Delta \mathbf{w}_k &\geq 0, & (42) \end{aligned}$$

is solved. Hence, no second-order information is required. This iterative procedure is combined with a globalization strategy (Nocedal and Wright,

2006) in order to achieve global convergence. The first-order information required to build the Jacobians of the cost and inequality constraints can be obtained by several methods (finite differences, automatic differentiation or symbolic calculations), however, due to the static characteristic of the cost in least squares problems and the inequality constraints, these Jacobians can be easily calculated by finite differences. On the other hand the Jacobian of the equality constraints, imposed by the dynamic model, is obtained, in this study, by using an ODE solver with sensitivity generation capabilities (Hindmarsh et al., 2005). This solver provides sensitivity information used to build the sparse and banded structure of Jacobian in the simultaneous Gauss-Newton method. Figure 4 shows the sparsity patterns in the Jacobians obtained by the multiple shooting parameterization for a PEP involving a dynamic model with 2 states, 3 parameters, 4 measurement points and bound constraints on the parameters. The sparse and banded structures in the formulation can be either exploited by sparse solvers or a condensing strategy can be applied in order to reduce the size of the matrices. This procedure leads to a smaller least squares problem involving dense matrices as described in Bock and Plitt (1984).

## 5. Case Studies

In the following, the multiple shooting parameterization is used to estimate the parameters in three benchmark case studies. Comparative results are illustrated for an arbitrary initialization against an initialization based on the solution of the convex modification (12)-(15).

### *5.1. Catalytic cracking of gas oil*

The first case study involves the catalytic cracking of gas oil A, to gasoline Q, and other products S (Tjoa and Biegler, 1991). The overall reaction scheme is represented by:

$$\begin{array}{ccc} & \overset{k_1}{\longrightarrow} & \\ \mathrm{A} & & \mathrm{Q} \\ {\scriptstyle k_3}\searrow & & \swarrow{\scriptstyle k_2} \\ & \mathrm{S} & \end{array} \tag{43}$$

The dynamics of the concentration of gas oil $x_1(t)$, and gasoline concentration $x_2(t)$, is described by the set nonlinear differential equations (45)-(46) and characterized by the three reaction rates $k_1$, $k_2$ and $k_3$. By defining the parameter vector as $p = [k_1,\ k_2,\ k_3]$, the PEP for this case study can be formulated as:

$$\min_{p,x(.)} \mathcal{J} = \frac{1}{2} \sum_{i=0}^{20} \sum_{j=1}^{2} \left( x_j(t_i) - \bar{x}_j(t_i) \right)^2 \tag{44}$$

subject to:

$$\begin{aligned} \dot{x}_1(t) &= -(k_1 + k_3) x_1^2, & (45) \\ \dot{x}_2(t) &= k_1 x_1^2 - k_2 x_2, & (46) \\ x_1(t_0) &= 1, & (47) \\ x_2(t_0) &= 0, & (48) \\ 0 &\leq k_1, k_2, k_3 \leq 20. & (49) \end{aligned}$$

The optimization problem arisen from the estimation of the reaction rates has been previously used as a benchmark to test optimization methods in Singer and Barton (2006) and Papamichail and Adjiman (2002), among others. Figure 5 depicts the set of noisy states measurements used for the estimation procedure and obtained from Floudas et al. (1999).

In order to visualize the complexity of the PEP, Figure 6 shows the cost in (44) when the parameters $k_1$ and $k_2$ are evaluated over a grid of points in the box $[0,\ 20] \times [0,\ 20]$. Although the problem is linear in parameters, the cost function is nonconvex in the optimization variables due to the nonlinearities in the states.

The constrained PEP (44)-(49) is parameterized using the multiple shooting approach by introducing shooting nodes at each measurement point, i.e., 21 shooting nodes and 3 parameters are considered as optimization variables. The resulting NLP is solved using a SQP routine with a quadratic programming (QP) solver based on an active set method.

In the first case, nodes are initialized with measurement points and the parameters take an arbitrary initialization. Assuming no-knowledge of a better initial guess for the parameter vector, the reaction rates are set to the center of the cube defined by the bound constraints (49), i.e., $p^0 = [10,\ 10,\ 10]^T$. This initialization leads to the optimum value $p^* = [12.2155,\ 7.9802,\ 2.2210]^T$ in four SQP iterations. In the second case, the optimization problem is convexified by using the presented approach, leading to a linear least squares problem of the form:

$$\min_{\tilde{p},\tilde{x}(.)} \tilde{\mathcal{J}} = \frac{1}{2} \sum_{i=0}^{20} \sum_{j=1}^{2} \left( \tilde{x}_j(t_i) - \bar{x}_j(t_i) \right)^2 \tag{50}$$

subject to

$$\begin{aligned} \dot{\bar{x}}_1(t) &= -(k_1 + k_3)\bar{x}_1^2, && (51)\\ \dot{\bar{x}}_2(t) &= k_1\bar{x}_1^2 - k_2\bar{x}_2, && (52)\\ \tilde{x}_1(t_0) &= 1, && (53)\\ \tilde{x}_2(t_0) &= 0, && (54)\\ 0 &\leq k_1, k_2, k_3 \leq 20. && (55) \end{aligned}$$

Since (50)-(55) is convex, initialization is not an issue and the problem is solved using a linear least squares solver based on the Gauss-Newton method. Hereafter, the obtained parameter solution, $p^*_{\mathrm{CVX}} = [8.0982,\ 6.3512,\ 3.4722]^T$, is used to initialize the original nonconvex optimization problem parameterized with the multiple shooting approach. The convex initialization leads to the same optimum $p^*$ previously presented. Consequently, the initial guess of the parameter vector $p^0$ is automatically calculated by the proposed method. Table 1 presents some relevant optimization parameters along with the results obtained from solution of the PEP (50)-(55). The algorithm parameters $\mathrm{TOL}_{\mathrm{SQP}}$, $\mathrm{ATOL}_{\mathrm{ODE}}$, $\mathrm{RTOL}_{\mathrm{ODE}}$ and $\mathrm{KKT}_{\mathrm{TOL}}$ correspond to the stopping value for the KKT tolerance, the absolute and relative tolerance of the ODE solver, and the KKT tolerance at the last iteration. Notice that $N_{\mathrm{Iter}}$, corresponding to the total number of SQP iterations, does not include the first iteration needed for the convex initialization in the proposed approach.

Figure 7 illustrates the convergence results for the problem with an arbitrary initialization and the ones obtained with the proposed methodology. It can be noticed that, in this particular case, the arbitrary initialization already provides a guess close to the optimum and the difference on convergence rates is not significant. However, the advantage of the proposed approach lies in the fact that no guess has to be proposed a priori.

### *5.2. Lotka-Volterra equations*

Consider the Lotka-volterra model independently introduced by Alfred J. Lotka in 1925 and Vito Volterra in 1926. The nonlinear differential equations (57)-(58) describe the time evolution of the population density for two species in a biological system, a predator $x_2(t)$ and its prey $x_1(t)$. The dynamic behavior of this interaction is characterized by the following parameters:

$\alpha$: intrinsic rate of prey population increase,
$\beta$: predation rate coefficient,

$\gamma$: reproduction rate of predators per 1 prey eaten,
$\delta$: predator mortality rate,

leading to a parameter vector $p = [\alpha,\ \beta,\ \gamma,\ \delta]^T$. Equations (57)-(58) exhibit two fixed points $[0, 0]$ and $[\alpha/\beta, \gamma/\delta]$. The first one corresponds to a saddle point while the second one to a center-stable, generating periodic solutions with an amplitude dependent on initial values. The oscillatory behavior of this pair of nonlinear equations is illustrated in Figure 8, where a set of noisy states measurements is obtained by simulating the model with nominal parameters $p = [0.6,\ 0.5,\ 0.7,\ 0.4]^T$, $x(t_0) = [1,\ 0.5]^T$ and adding Gaussian noise with a variance $\sigma^2 = 0.05$. This benchmark problem can be found in Floudas et al. (1999) where only two of the four parameters are estimated.

Although the system (57)-(58) is parameter-affine, the estimation of the parameter vector $p$ is not a simple task. The PEP can be formulated as:

$$\min_{p,x(.)} \mathcal{J} = \frac{1}{2} \sum_{i=0}^{20} \sum_{j=1}^{2} \left(x_j(t_i) - \bar{x}_j(t_i)\right)^2 \tag{56}$$

subject to

$$\begin{aligned} \dot{x}_1(t) &= \alpha x_1 - \beta x_1 x_2, & (57)\\ \dot{x}_2(t) &= -\gamma x_2 + \delta x_1 x_2, & (58)\\ 0 &\leq \alpha, \beta, \gamma, \delta \leq 2, & (59) \end{aligned}$$

where $\bar{x}(t_i)$ represents the noisy state measurements in Figure 8. The contaminated data sequence is used to evaluate the cost (56) when the pair $[\alpha\ \gamma]$ changes while the parameters $\beta$ and $\delta$ remain constant and equal to their original values. Figure 9 presents the obtained nonconvex cost as a function of the varied parameters for a fixed initial condition $[x_1(t_0), x_2(t_0)]^T = [1, 0.5]^T$. Notice that in this case a local minimum can be easily attained by the unappropriated initialization of the problem.

The PEP is parameterized using the DMS approach using the same procedure as in the first study case. In this example 21 shooting nodes are optimized along with the four model parameters $\alpha$, $\beta$, $\gamma$ and $\delta$. Initialization of the parameter vector $p$ is arbitrarily performed first by setting the initial guess to the center of the hyperbox defined by the bounds constraints (59), i.e, $p^0 = [1, 1, 1, 1]^T$. This initialization leads to an optimal value $p^* = [0.6700,\ 0.5455,\ 0.6288,\ 0.3501]^T$. In a second test, the initialization is performed with the value $p^*_{\text{CVX}} = [0.6343, 0.483, 0.5617, 0.288]^T$,

corresponding to the solution of the convex optimization problem described by

$$\min_{p,\tilde{x}(.)} \tilde{\mathcal{J}} = \frac{1}{2} \sum_{i=0}^{20} \sum_{j=1}^{2} \left( \tilde{x}_j(t_i) - \bar{x}_j(t_i) \right)^2 \tag{60}$$

subject to

$$\begin{aligned} \dot{\tilde{x}}_1(t) &= \alpha \bar{x}_1 - \beta \bar{x}_1 \bar{x}_2, & (61) \\ \dot{\tilde{x}}_2(t) &= -\gamma \bar{x}_2 + \delta \bar{x}_1 \bar{x}_2, & (62) \\ 0 &\leq \alpha, \beta, \gamma, \delta \leq 2, & (63) \end{aligned}$$

and leads to the same optimum obtained with the arbitrary initialization. Table 2 summarizes algorithm parameters along with the results obtained with both approaches. Additionally, Figure 10 illustrates the performance of both approaches, where it is possible to appreciate faster convergence of the SGN method with the convex initialization. Notice that in the second iteration, continuity conditions are almost totally satisfied.

*5.3. Complex Batch Reaction*

The batch reaction of formaldehyde, $A$, and sodium $p$-phenol sulfonate, $B$, exhibits a complex dynamic scheme with four intermediates, $C, D, F$ and $G$, and a final product, $E$. All the reactions follow second-order kinetics and are modeled as proposed in Ingham et al. (2000). Table 3 illustrates the reactions, their rates and nominal values. In order to simplify the notation, the concentration of the reactants, products and intermediates, $A$ to $G$ are represented by $x_1(t)$ to $x_7(t)$, respectively and the parameter vector is defined as $p = [k_1, \ldots, k_8]$. The parameter estimation problem can be cast as

$$\min_{p,x(.)} \mathcal{J} = \frac{1}{2} \sum_{i=0}^{10} \sum_{j=1}^{7} \left( x_j(t_i) - \bar{x}_j(t_i) \right)^2 \tag{64}$$

subject to

$$\begin{aligned} \dot{x}_1(t) &= -k_1 x_1 x_2 - k_2 x_1 x_3 - k_7 x_1 x_7 - k_8 x_1 x_6, & (65) \\ \dot{x}_2(t) &= -k_1 x_1 x_2 - k_4 x_2 x_4 - k_6 x_3 x_2, & (66) \\ \dot{x}_3(t) &= k_1 x_1 x_2 - k_2 x_1 x_3 - k_3 x_3 x_4 - 2k_5 x_3^2 \\ &\quad -k_6 x_3 x_2, & (67) \end{aligned}$$

$$
\begin{aligned}
\dot{x}_4(t) &= k_2 x_1 x_3 - k_3 x_3 x_4 - k_4 x_2 x_4, && (68)\\
\dot{x}_5(t) &= k_3 x_3 x_4 + k_8 x_1 x_6, && (69)\\
\dot{x}_6(t) &= k_4 x_2 x_4 + k_5 x_3^2 + k_7 x_1 x_7 - k_8 x_1 x_6, && (70)\\
\dot{x}_7(t) &= k_6 x_3 x_2 - k_7 x_1 x_7, && (71)\\
0 &\leq k_1, k_2, \ldots, k_8 \leq 1, && (72)\\
0 &\leq x_1, \ldots, x_7. && (73)
\end{aligned}
$$

Figure 11 shows the noisy state measurements $\bar{x}(t_i)$, obtained when (65) to (71) are solved with the initial condition $x(t_0) = [0.15, 0.1, 0, 0, 0, 0, 0]^T$. This data set has been contaminated with Gaussian noise with standard deviation $\sigma = 1 \times 10^{-3}$ for $x_1$, $x_2$, $x_3$ and $x_5$ and $\sigma = 2.23 \times 10^{-4}$ for $x_4$, $x_6$ and $x_7$[5].

Figure 12 illustrates the nonconvex cost (64) when 6 parameters are fixed and the initial condition is set to the one introduced previously. It is not difficult to see that despite the linearity in the parameters, the optimization problem becomes nonconvex due to the nonlinearity in the states.

The PEP (64)-(72) is parameterized using the DMS approach and solved with initialization of the shooting nodes at the measurement points and arbitrarily setting $p^0 = [1,\ 1,\ 1,\ 1,\ 1,\ 1,\ 1,\ 1]^T$. In this case, it takes eight iterations to reach the optimum $p^* = [162.03,\ 41.13,\ 142.57,\ 32.87,\ 44.71,\ 57.46,\ 50.33,\ 54.91]^T \times 10^{-3}$. In order to improve convergence rate and avoid arbitrary initialization, the proposed approach is applied and the convex problem

$$
\min_{p,\tilde{x}(.)} \mathcal{J}_c = \frac{1}{2} \sum_{i=0}^{10} \sum_{j=1}^{7} \left( \tilde{x}_j(t_i) - \bar{x}_j(t_i) \right)^2 \qquad (74)
$$

subject to:

$$
\begin{aligned}
\dot{\tilde{x}}_1(t) &= -k_1 \bar{x}_1 \bar{x}_2 - k_2 \bar{x}_1 \bar{x}_3 - k_7 \bar{x}_1 \bar{x}_7 - k_8 \bar{x}_1 \bar{x}_6, && (75)\\
\dot{\tilde{x}}_2(t) &= -k_1 \bar{x}_1 \bar{x}_2 - k_4 \bar{x}_2 \bar{x}_4 - k_6 \bar{x}_3 \bar{x}_2, && (76)\\
\dot{\tilde{x}}_3(t) &= k_1 \bar{x}_1 \bar{x}_2 - k_2 \bar{x}_1 \bar{x}_3 - k_3 \bar{x}_3 \bar{x}_4 - 2k_5 \bar{x}_3^2 \\
&\quad -k_6 \bar{x}_3 \bar{x}_2, && (77)\\
\dot{\tilde{x}}_4(t) &= k_2 \bar{x}_1 \bar{x}_3 - k_3 \bar{x}_3 \bar{x}_4 - k_4 \bar{x}_2 \bar{x}_4, && (78)\\
\dot{\tilde{x}}_5(t) &= k_3 \bar{x}_3 \bar{x}_4 + k_8 \bar{x}_1 \bar{x}_6, && (79)
\end{aligned}
$$

[5]Different levels of noise are used due to different amplitudes in the states trajectories

$$\dot{\bar{x}}_6(t) = k_4\bar{x}_2\bar{x}_4 + k_5\bar{x}_3^2 + k_7\bar{x}_1\bar{x}_7 - k_8\bar{x}_1\bar{x}_6, \quad (80)$$

$$\dot{\bar{x}}_7(t) = k_6\bar{x}_3\bar{x}_2 - k_7\bar{x}_1\bar{x}_7, \quad (81)$$

$$0 \leq k_1, k_2, \ldots, k_8 \leq 1, \quad (82)$$

$$0 \leq \tilde{x}_1, \ldots, \tilde{x}_7, \quad (83)$$

is solved first. The obtained solution $p^*_{\mathrm{CVX}} = [112.6,\ 30.4,\ 125.6,\ 0,\ 42.4,\ 33.7,\ 30.5,\ 49.9]^T \times 10^{-3}$ is used to initialize the SGN algorithm, leading to the same optimal value previously presented. Table 4 summarizes some of the algorithm parameters along with the parameter optimization results for this study case.

Figure 13 illustrates the evolution of the iterations for the methods with arbitrary initialization and the proposed approach. The state evolution of the intermediate compounds is not presented for clarity in the visualization. Note also that while convergence is achieved after the fourth iteration when the problem is arbitrarily initialized, the SGN with the proposed convex initialization method already attains convergence after the first iteration. Consequently, the advantage of the presented methodology lies not only in improving the convergence speed but in the fact that no arbitrary initialization is performed and the initial value is calculated by solving a related convex problem.

## 6. Conclusion

An initialization method for the solution of parameter estimation problems in nonlinear parameter-affine dynamic models has been presented. An assessment of the solution errors is presented showing that the they are of second order in the size of the perturbations. Three benchmark examples has been studied, illustrating that the heuristic of the method reduces the number of iteration required to converge to a solution. The advantages of the method not only lie in improving convergence properties but also in the fact that no previous knowledge of an initial guess for the parameter vector is required, allowing an automatic initialization by using the power of the convex optimization.

## 7. Acknowledgments

Research supported by Research Council KUL:OT/03/30, CoE EF/05/006 Optimization in Engineering(OPTEC), GOA AMBioRICS, IOF-SCORES4CHEM,

PhD/postdoc and fellow grants; Flemish Government: FWO: PhD/postdoc grants, projects G.0452.04, G.0499.04, G.0211.05, G.0226.06, G.0321.06, G.0302.07, G.0320.08, G.0558.08, G.0557.08, G.0588.09, research communities (ICCoS, ANMMM, MLDM); G.0377.09; IWT: PhD Grants, McKnow-E, Eureka-Flite+, SBO LeCoPro, SBO Climaqs; Helmholtz: viCERP, ACCM, Bauknecht, Hoerbiger; EU: ERNSI,HD-MPC; Contracts: AMINAL; Belgian Federal Science Policy Office: IUAP P6/04 (DYSCO, Dynamical systems, control and optimization, 2007-2011).

## References

Biegler, L. T., 1984. Solution of dynamic optimization problems by successive quadratic programming and orthogonal collocation. Computers & Chemical Engineering. 8 (3/4), 243–248.

Biegler, L. T., Cervantes, A. M., Wachter, A., 2002. Advances in simultaneous strategies for dynamic process optimization. Chemical Engineering Science 57 (4), 575–593.

Bock, H., Plitt, K., 1984. A multiple shooting algorithm for direct solution of optimal control problems. In: Proc. 9th IFAC world congress. Budapest, Hungary, pp. 242–247.

Bonilla, J., Diehl, M., De Moor, B., Van Impe, J., 2008. A nonlinear least squares estimation procedure without initial parameter guesses. In: Proc. of the 47th IEEE Conference on Decision and Control (CDC'08). Cancún, México, pp. 5519–5524.

Bonilla, J., Diehl, M., Logist, F., De Moor, B., Van Impe, J., 2007. A convexity-based homotopy method for nonlinear optimization in model predictive control. SISTA Internal Report 07-226, Katholieke Universiteit Leuven, Electrical Engineering Department.

Bonilla, J., Diehl, M., Logist, F., De Moor, B., Van Impe, J., 2009. A convex approximation for parameter estimation involving parameter-affine dynamic models. SISTA Internal Report 09-52, Katholieke Universiteit Leuven, Electrical Engineering Department.

Boyd, S., Vandenberghe, L., 2006. Convex Optimization, 1st Edition. Cambridge University Press, Cambridge.

Cervantes, A., Biegler, L. T., 1999. Optimization strategies for dynamic systems. In: Floudas, C., Pardalos, P. (Eds.), Encyclopedia of Optimization. Kluwer Academic Publishers, Dordrecht, The Netherlands.

Diehl, M., 2001. Real-time optimization for large scale nonlinear processes. Ph.D. thesis, University of Heidelberg, [Online] http://www.iwr.uni-heidelberg.de/%7EMoritz.Diehl/DISSERTATION/index.html.

Floudas, C. A., Pardalos, P. M., Adjiman, C. S., Esposito, W. R., Gumus, Z. H., Harding, S. T., Klepeis, J. L., Meyer, C. A., Schweiger, C. A., 1999. Handbook of test problems in local and global optimization. In nonconvex optimization and its applications. Kluwer Academic Publishers, Dordrecht, The Netherlands.

Gould, N., 1989. On the convergence of sequential penalty function methods for constrained minimization. SIAM Journal of Numerical Analysis 26 (1), 107–128.

Hindmarsh, A. C., Brown, P. N., Grant, K. E., Lee, S. L., Serban, R., Shumaker, D. E., , Woodward, C. S., 2005. SUNDIALS: Suite of nonlinear and differential/algebraic equation solvers. ACM Transactions on Mathematical Software 31 (3), 363–396.

Ingham, H., Dunn, I. J., Heinzle, E., Přenosil, J. E., 2000. Chemical Engineering Dynamics: An Introduction to modelling and computer simulation, 2nd Edition. Wiley-VCH, Weinheim, Germany.

Kostina, E., 2004. Robust parameter estimation in dynamic systems. Optimization and Engineering 5 (4), 461–484.

Ljung, L., 1999. System Identification, Theory for the Users, 2nd Edition. Prentice Hall, New Jersey.

Ljung, L., 2002. Prediction error estimation methods. Circuits Systems & Signal Processing 21 (1), 11–21.

Nocedal, J., Wright, S., 2006. Numerical Optimization, 2nd Edition. Springer, New York.

Papamichail, I., Adjiman, C. S., 2002. A rigorous global optimization algorithm for problems with ordinary differential equations. Journal of Global Optimization 24 (1), 1–33.

Pontryagin, L. S., 1962. The Mathematical Theory of Optimal Processes. Interscience Publishers, New York.

Robinson, S., 1982. Generalized equations and their solutions II. applications to nonlinear programming. Mathematical Programming Studies 19 (19), 200–221.

Singer, A. B., Barton, P. I., 2006. Global optimization with nonlinear ordinary differential equations. Journal of Global Optimization (34), 159–190.

Tjoa, I. B., Biegler, L. T., 1991. Simultaneous solution and optimization strategies for parameter estimation of differential-algebraic equation systems. Industrial & Engineering Chemistry Research 30, 376–385.

Watson, L. T., 2000. Theory of globally convergent probability-one homotopies for nonlinear programming. SIAM Journal on Optimization 11 (3), 761–780.

## A. Proof of Lemma 2

Notice that in view of Lemma 1, $\bar{\bar{p}}$ is the solution of the convex unperturbed problem. Consequently, it is enough to prove that the distance between the unperturbed solution of the convex problem and its perturbed one obeys (25). In order to do so, consider the PEP

$$\min_{p,\mathbf{x}} \frac{1}{2}\|\mathbf{x}-\hat{\mathbf{x}}\|_Q^2 \quad \text{s.t.} \quad A(\hat{\mathbf{x}}) - B(\hat{\mathbf{x}})p - W\mathbf{x} = \mathbf{0}, \tag{84}$$

which corresponds to the convex problem for unperturbed ($\hat{\mathbf{x}} = \bar{\bar{\mathbf{x}}}$) and perturbed ($\hat{\mathbf{x}} = \bar{\mathbf{x}}$) measurements. Notice that the inequality constraints can be neglected for $\hat{\mathbf{x}} = \bar{\bar{\mathbf{x}}}$ due to Corollary 1. Additionally, for sufficiently small perturbations, the inequality constraints remain inactive, this allows to neglect the inequality constraints when $\hat{\mathbf{x}} = \bar{\mathbf{x}}$. Consequently, the convex formulation is reduced to (84) for the unperturbed measurement set and in a small neighborhood of it $\|\bar{\bar{\mathbf{x}}} - \bar{\mathbf{x}}\| \leq \epsilon$, $\epsilon > 0$.

The Karush-Kuhn-Tucker (KKT) optimality conditions for (84) yield:

$$F(\mathbf{x}^*, p^*, \lambda^*, \hat{\mathbf{x}}) = \begin{bmatrix} Q & \mathbf{0} & -W^T \\ \mathbf{0} & \mathbf{0} & -B(\hat{\mathbf{x}})^T \\ -W & -B(\hat{\mathbf{x}}) & \mathbf{0} \end{bmatrix} \begin{bmatrix} \mathbf{x}^* \\ p^* \\ \lambda^* \end{bmatrix} - \begin{bmatrix} Q\hat{\mathbf{x}} \\ \mathbf{0} \\ -A(\hat{\mathbf{x}}) \end{bmatrix} = \mathbf{0}. \tag{85}$$

which provides the solution $(\mathbf{x}^*(\hat{\mathbf{x}}), p^*(\hat{\mathbf{x}}), \lambda^*(\hat{\mathbf{x}}))$ for the perturbed problem $\hat{\mathbf{x}} = \bar{\mathbf{x}}$ and the unperturbed one $\hat{\mathbf{x}} = \bar{\bar{\mathbf{x}}}$. Under the small perturbation condition, the change in the solutions given a change in the measurement data is given by

$$\begin{bmatrix} \frac{\partial \mathbf{x}^*(\hat{\mathbf{x}})}{\partial \hat{\mathbf{x}}} \\ \frac{\partial p^*(\hat{\mathbf{x}})}{\partial \hat{\mathbf{x}}} \\ \frac{\partial \lambda^*(\hat{\mathbf{x}})}{\partial \hat{\mathbf{x}}} \end{bmatrix} = \begin{bmatrix} Q & \mathbf{0} & -W^T \\ \mathbf{0} & \mathbf{0} & -B(\hat{\mathbf{x}})^T \\ W & -B(\hat{\mathbf{x}}) & \mathbf{0} \end{bmatrix}^{-1} \tag{86}$$
$$\left\{ \begin{bmatrix} \mathbf{0} & \mathbf{0} & \mathbf{0} \\ \mathbf{0} & \mathbf{0} & -\frac{\partial B(\hat{\mathbf{x}})^T}{\partial \hat{\mathbf{x}}} \\ \mathbf{0} & -\frac{\partial B(\hat{\mathbf{x}})}{\partial \hat{\mathbf{x}}} & \mathbf{0} \end{bmatrix} \begin{bmatrix} \mathbf{x}^*(\hat{\mathbf{x}}) \\ p^*(\hat{\mathbf{x}}) \\ \lambda^*(\hat{\mathbf{x}}) \end{bmatrix} + \begin{bmatrix} Q \\ \mathbf{0} \\ \frac{\partial A(\hat{\mathbf{x}})}{\partial \hat{\mathbf{x}}} \end{bmatrix} \right\}.$$

Due to assumptions A1 to A3, the Jacobian of $F(\mathbf{x}^*, p^*, \lambda^*, \hat{\mathbf{x}})$ is invertible at $(\bar{\bar{\mathbf{x}}}, \bar{\bar{p}}, \bar{\bar{\lambda}})$. Moreover, the perturbed Jacobian remains invertible for small changes in the measurement data $\|\bar{\mathbf{x}} - \bar{\bar{\mathbf{x}}}\|$. Consequently, the change in the optimal values also depends on the size of the perturbation as can be inferred from the smoothness of the involved functions in (86).

## B. Proof of Theorem 1

In order to simplify the notation, the following definitions are introduced:

$$\mathbf{w} = [\mathbf{x}^T, p^T]^T, \quad Q_{\mathbf{w}} = \begin{bmatrix} Q & 0 \\ 0 & 0 \end{bmatrix}. \tag{87}$$

Consider the original PEP with the set of perturbed measurements $\bar{\mathbf{x}}$. Following Corollary 1, the original PEP can be formulated as:

$$\mathrm{PEP}_{\mathrm{NL}}(\bar{\mathbf{w}}): \quad \min_{\mathbf{w}} \frac{1}{2}\|\mathbf{w}-\bar{\mathbf{w}}\|^2_{Q_{\mathbf{w}}} \tag{88}$$

subject to

$$g(\mathbf{w}) = 0. \tag{89}$$

Notice that Corollary 1 implies that the inequality constraints can be neglected for $\|\bar{\bar{\mathbf{x}}}-\bar{\mathbf{x}}\|$ small enough. Now, the KKT conditions for the quadratic programming problem:

$$\mathrm{PEP}_{\mathrm{LIN}}(\bar{\mathbf{w}},\hat{\mathbf{w}}): \quad \min_{\mathbf{w}} \frac{1}{2}\|\mathbf{w}-\bar{\mathbf{w}}\|^2_{Q_{\mathbf{w}}} \tag{90}$$

subject to

$$g(\hat{\mathbf{w}}) + \nabla g(\hat{\mathbf{w}})^T(\mathbf{w}-\hat{\mathbf{w}}) = 0, \tag{91}$$

at the linearization point $\tilde{\mathbf{w}}$ are considered, i.e.,

$$F(\mathbf{w},\lambda,\bar{\mathbf{w}},\tilde{\mathbf{w}}) = \begin{bmatrix} Q_{\mathbf{w}}(\mathbf{w}-\bar{\mathbf{w}}) + \nabla g(\hat{\mathbf{w}})\lambda \\ g(\hat{\mathbf{w}}) + \nabla g(\hat{\mathbf{w}})^T(\mathbf{w}-\hat{\mathbf{w}}) \end{bmatrix} = \mathbf{0}, \tag{92}$$

where $\lambda$ represents the Lagrange multipliers for the equality constrained problem. This set of equations provides a solution $\mathbf{w}^*_{\mathrm{LIN}}(\bar{\mathbf{w}},\hat{\mathbf{w}})$ as a function of the linearization point and the set of measurements.

For sufficiently small perturbations $\|\bar{\mathbf{x}}-\bar{\bar{\mathbf{x}}}\|$ and considering assumptions A1 to A3 it is possible to establish the following relations

$$\mathrm{A}: \|\mathbf{w}^*(\bar{\mathbf{w}}) - \mathbf{w}^*_{\mathrm{LIN}}(\bar{\mathbf{w}},\bar{\bar{\mathbf{w}}})\| = \mathcal{O}(\|\bar{\mathbf{w}}-\bar{\bar{\mathbf{w}}}\|^2) \tag{93}$$

and

$$\|\mathbf{w}^*_{\mathrm{LIN}}(\bar{\mathbf{w}},\bar{\bar{\mathbf{w}}}) - \bar{\bar{\mathbf{w}}}\| = \mathcal{O}(\|\bar{\mathbf{w}}-\bar{\bar{\mathbf{w}}}\|) \tag{94}$$

Equation (93) states that the solution provided by the first-order predictor $\mathbf{w}^*_{\mathrm{LIN}}(\bar{\mathbf{w}},\bar{\bar{\mathbf{w}}})$ differs from the real solution $\mathbf{w}^*(\bar{\mathbf{w}})$ by $\mathcal{O}(\|\bar{\mathbf{w}}-\bar{\bar{\mathbf{w}}}\|^2)$ as presented in (Diehl, 2001, Theorem 3.6 and section 3.4.1). Equation (94) is a result of perturbation analysis of optimization problems (Robinson, 1982) under assumption A1 to A3 and can be easily proved by linearizing the original problem around the unperturbed solution.

Considering (93) and (94), Theorem 1

$$\mathrm{C}: \|\mathbf{w}^*(\bar{\mathbf{w}}) - \mathbf{w}^*_{\mathrm{LIN}}(\bar{\mathbf{w}},\mathbf{w}^*_{\mathrm{cvx}})\| = \mathcal{O}(\|\bar{\mathbf{x}}-\bar{\bar{\mathbf{x}}}\|^2) \tag{95}$$

is proven by showing that the distance between the first-order predictor solution $\mathbf{w}^*_{\text{LIN}}(\bar{\mathbf{w}}, \bar{\bar{\mathbf{w}}})$ and the solution provided by $\mathbf{w}^*_{\text{LIN}}(\bar{\mathbf{w}}, \mathbf{w}^*_{\text{cvx}})$ is of second-order in $\|\bar{\mathbf{w}} - \bar{\bar{\mathbf{w}}}\|$, i.e.,

$$\text{B} : \|\mathbf{w}^*_{\text{LIN}}(\bar{\mathbf{w}}, \bar{\bar{\mathbf{w}}}) - \mathbf{w}^*_{\text{LIN}}(\bar{\mathbf{w}}, \mathbf{w}^*_{\text{cvx}})\| = \mathcal{O}(\|\bar{\mathbf{w}} - \bar{\bar{\mathbf{w}}}\|^2). \tag{96}$$

Notice that in this proof what is basically used is a inequality triangle, i.e., A&B $\Rightarrow$ C. Consequenlty C is proved by proving B. In order to do so, consider the series expansion of the linear predictor solution around the minimizer provided by the convex problem using the perturbed set of measurements[6],

$$\begin{aligned} \mathbf{w}^*_{\text{LIN}}(\bar{\mathbf{w}}, \mathbf{w}^*_{\text{cvx}}) &= \mathbf{w}^*_{\text{LIN}}(\bar{\mathbf{w}}, \bar{\bar{\mathbf{w}}}) \\ &\quad + \frac{\partial \mathbf{w}^*_{\text{LIN}}(\bar{\mathbf{w}}, \hat{\mathbf{w}})}{\partial \hat{\mathbf{w}}} \mid_{\hat{\mathbf{w}}=\bar{\bar{\mathbf{w}}}} (\mathbf{w}^*_{\text{cvx}} - \bar{\bar{\mathbf{w}}}) \\ &\quad + \mathcal{O}(\|\mathbf{w}^*_{\text{cvx}} - \bar{\bar{\mathbf{w}}}\|^2). \end{aligned} \tag{97}$$

The term

$$\frac{\partial \mathbf{w}^*_{\text{LIN}}(\bar{\mathbf{w}}, \hat{\mathbf{w}})}{\partial \hat{\mathbf{w}}} \mid_{\hat{\mathbf{w}}=\bar{\bar{\mathbf{w}}}} (\mathbf{w}^*_{\text{cvx}} - \bar{\bar{\mathbf{w}}}) \tag{98}$$

is investigated in detail. By evaluating (92) at the solution $(\mathbf{w}^*_{\text{LIN}}, \lambda^*_{\text{LIN}})$,

$$F(\mathbf{w}^*_{\text{LIN}}, \lambda^*_{\text{LIN}}, \bar{\mathbf{w}}, \hat{\mathbf{w}}) = 0, \tag{99}$$

and applying the implicit function theorem to it, it is possible to obtain an expression for the first factor in (98),

$$\frac{\partial \mathbf{w}^*_{\text{LIN}}(\bar{\mathbf{w}}, \hat{\mathbf{w}})}{\partial \hat{\mathbf{w}}} = -[\mathbb{I} \;\; 0] J(\hat{\mathbf{w}})^{-1} \frac{\partial F}{\partial \hat{\mathbf{w}}}, \tag{100}$$

with

$$\begin{aligned} J(\hat{\mathbf{w}}) &= \frac{\partial F(\mathbf{w}^*_{\text{LIN}}, \lambda^*_{\text{LIN}}, \bar{\mathbf{w}}, \hat{\mathbf{w}})}{\partial (\mathbf{w}^*_{\text{LIN}}, \lambda^*_{\text{LIN}})} \\ &= \begin{bmatrix} Q_{\mathbf{w}} & \nabla g(\hat{\mathbf{w}}) \\ \nabla g(\hat{\mathbf{w}})^T & 0 \end{bmatrix}, \end{aligned}$$

and

$$\frac{\partial F}{\partial \hat{\mathbf{w}}} = \begin{bmatrix} \nabla^2 g(\hat{\mathbf{w}}) \lambda^*_{\text{LIN}} \\ \nabla^2 g(\hat{\mathbf{w}})(\mathbf{w}^*_{\text{LIN}} - \hat{\mathbf{w}}) \end{bmatrix}. \tag{101}$$

[6]This linear predictor is the model used in the first SQP iteration.

Equation (100) is obtained by considering that $\frac{\partial \bar{\mathbf{w}}}{\partial \hat{\mathbf{w}}} = 0$, i.e., the measurement data does not depend on the linearization point. Assuming A3, and the invertibility of $J(\bar{\bar{\mathbf{w}}})$, at the linearization point ,$\hat{\mathbf{w}} = \bar{\bar{\mathbf{w}}}$, $J(\bar{\bar{\mathbf{w}}})^{-1}$ and $\nabla^2 g(\bar{\bar{\mathbf{w}}})$ become constants yielding

$$\frac{\partial \mathbf{w}^*_{\text{LIN}}(\bar{\mathbf{w}}, \hat{\mathbf{w}})}{\partial \hat{\mathbf{w}}}|_{\hat{\mathbf{w}}=\bar{\bar{\mathbf{w}}}} \;=\; \mathcal{O}\left( \left\| \begin{array}{c} \lambda^*_{\text{LIN}}(\bar{\mathbf{w}}, \bar{\bar{\mathbf{w}}}) \\ \mathbf{w}^*_{\text{LIN}}(\bar{\mathbf{w}}, \bar{\bar{\mathbf{w}}}) - \bar{\bar{\mathbf{w}}} \end{array} \right\| \right) \tag{102}$$

Note that $\mathbf{w}^*_{\text{LIN}}(\bar{\mathbf{w}}, \bar{\bar{\mathbf{w}}}) - \bar{\bar{\mathbf{w}}}$ corresponds to the distance between the unperturbed solution $\bar{\bar{\mathbf{w}}}$ and the perturbed one provided by the use of a linear predictor in the constraints. This distance is given by (94) and leads to

$$\frac{\partial \mathbf{w}^*_{\text{LIN}}(\bar{\mathbf{w}}, \hat{\mathbf{w}})}{\partial \hat{\mathbf{w}}}|_{\hat{\mathbf{w}}=\bar{\bar{\mathbf{w}}}} = \mathcal{O}(\|\bar{\mathbf{w}} - \bar{\bar{\mathbf{w}}}\|). \tag{103}$$

Hence, combining (103) and Lemma 2 yields

$$\frac{\partial \mathbf{w}^*_{\text{LIN}}(\bar{\mathbf{w}}, \hat{\mathbf{w}})}{\partial \hat{\mathbf{w}}} \,|_{\hat{\mathbf{w}}=\bar{\bar{\mathbf{w}}}} \,(\mathbf{w}^*_{\text{cvx}} - \bar{\bar{\mathbf{w}}}) = \mathcal{O}(\|\bar{\mathbf{w}} - \bar{\bar{\mathbf{w}}}\|^2) \tag{104}$$

Consequently, (97) is rewritten by using (104) leading to

$$\mathbf{w}^*_{\text{LIN}}(\bar{\mathbf{w}}, \mathbf{w}^*_{\text{cvx}}) = \mathbf{w}^*_{\text{LIN}}(\bar{\mathbf{w}}, \bar{\bar{\mathbf{w}}}) + \mathcal{O}(\|\mathbf{w}^*_{\text{cvx}} - \bar{\bar{\mathbf{w}}}\|^2), \tag{105}$$

i.e., the solutions $\mathbf{w}^*_{\text{LIN}}(\bar{\mathbf{w}}, \mathbf{w}_{\text{cvx}})$, and $\mathbf{w}^*_{\text{LIN}}(\bar{\mathbf{w}}, \bar{\bar{\mathbf{w}}})$ are identically apart from second order perturbations.

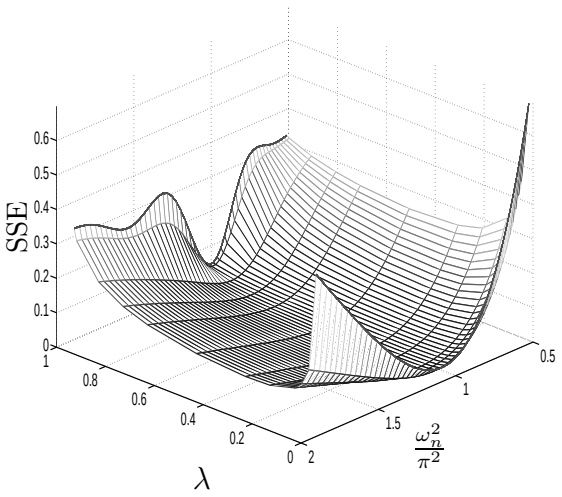


Figure 1:

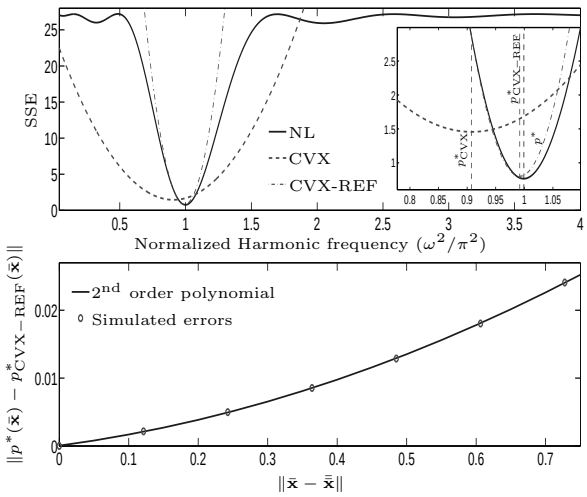


Figure 2:

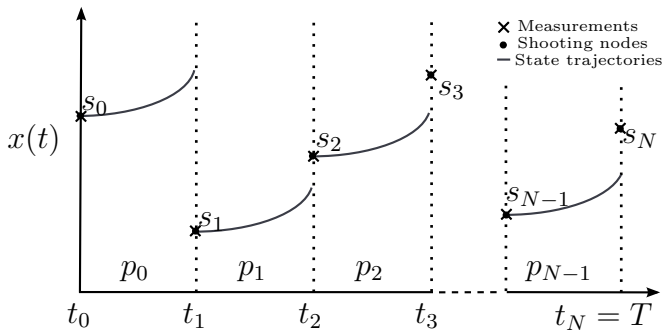
Measurements
Shooting nodes
State trajectories
$x(t)$
$s_0$
$s_1$
$s_2$
$s_3$
$s_{N-1}$
$s_N$
$p_0$
$p_1$
$p_2$
$p_{N-1}$
$t_0$
$t_1$
$t_2$
$t_3$
$t_N = T$

Figure 3:

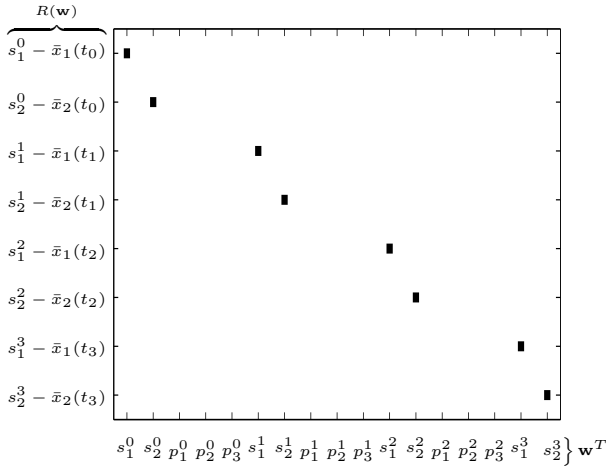


(a) Residuals cost Jacobian $\nabla R(\mathbf{w})^T$

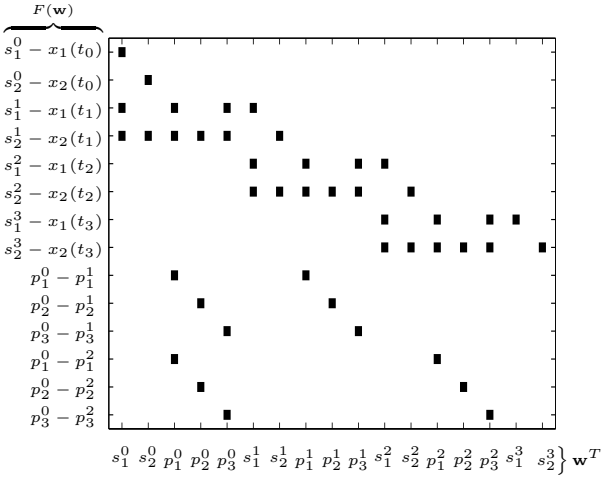


(b) Equality constraints Jacobian $\nabla F(\mathbf{w})^T$

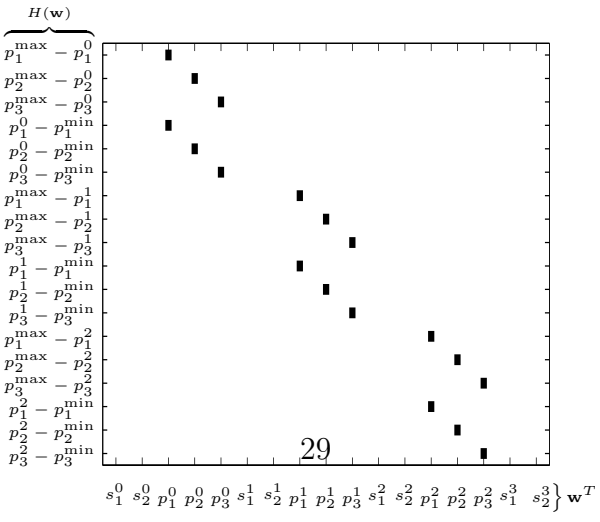




(c) Inequality constraints Jacobian $\nabla H(\mathbf{w})^T$

Figure 4:

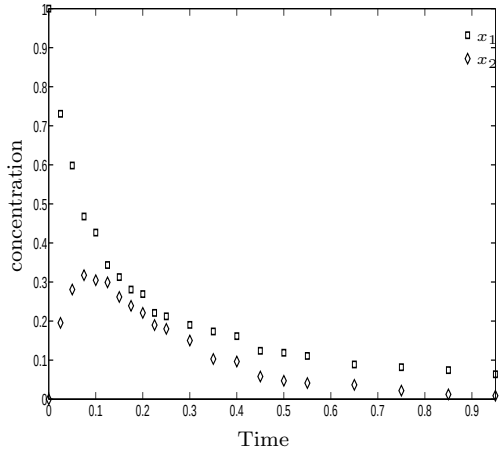


Figure 5:

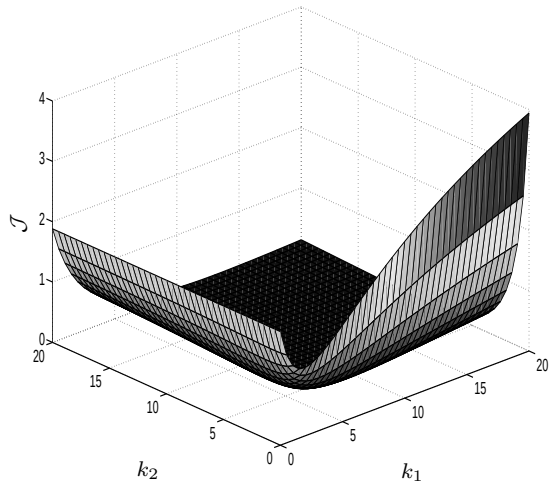


Figure 6:

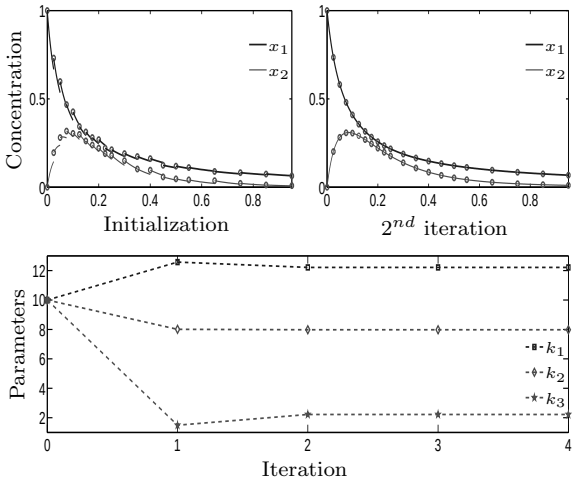


(a) Arbitrary initialization

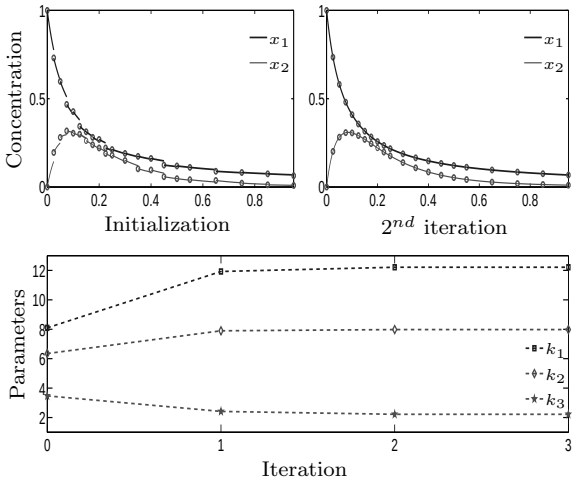


(b) Convex approach

Figure 7:

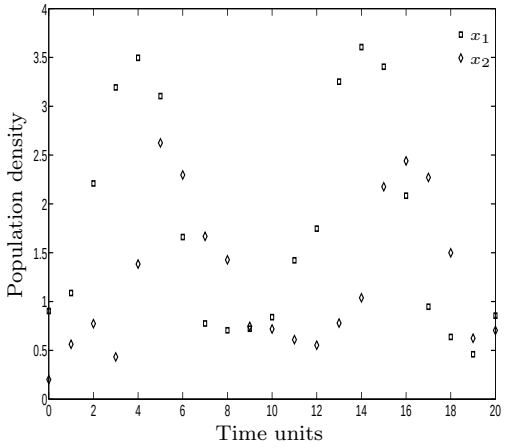


Figure 8:

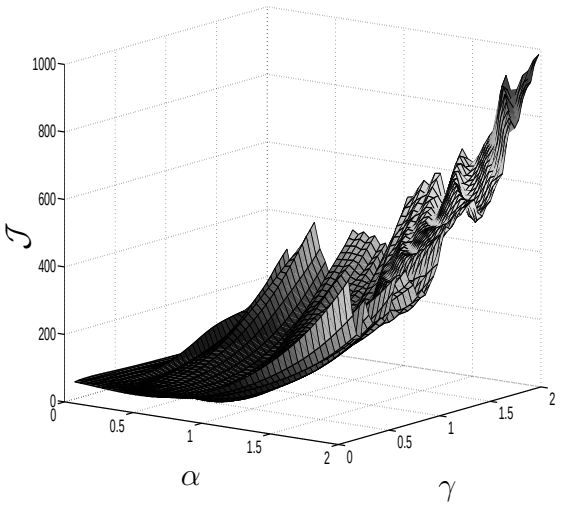


Figure 9:

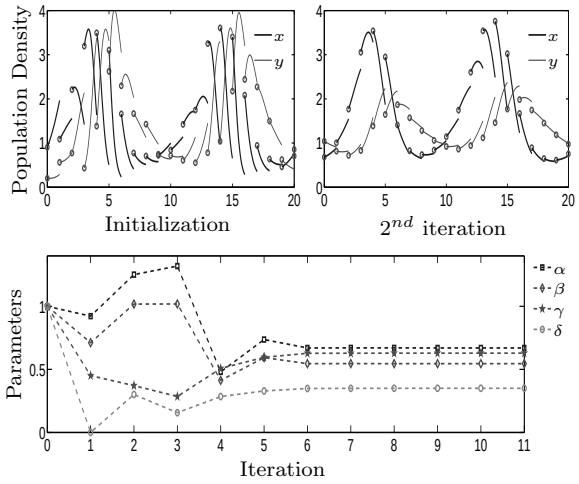


(a) Arbitrary initialization

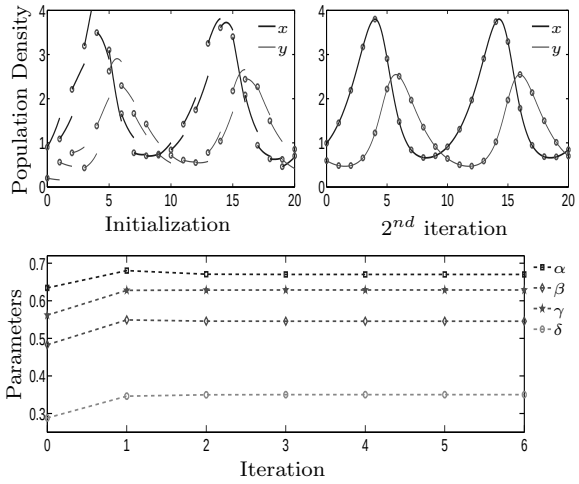


(b) Convex approach

Figure 10:

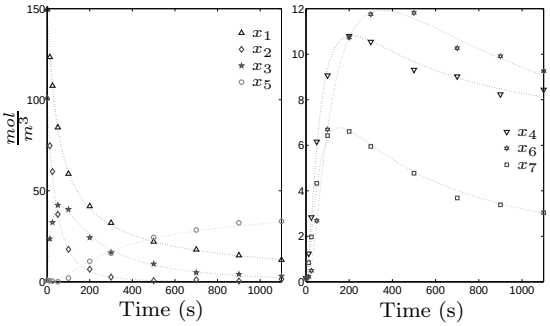


Figure 11:

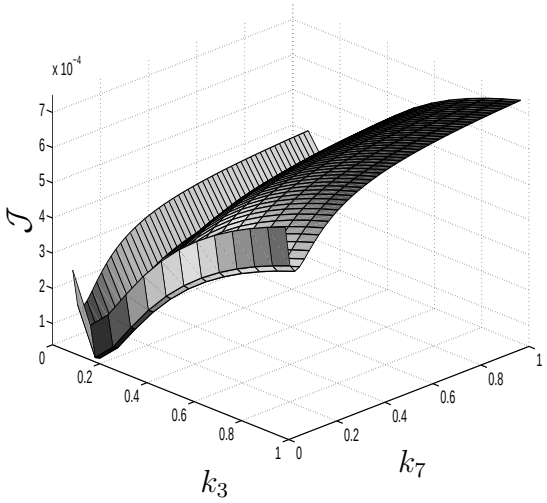


Figure 12:

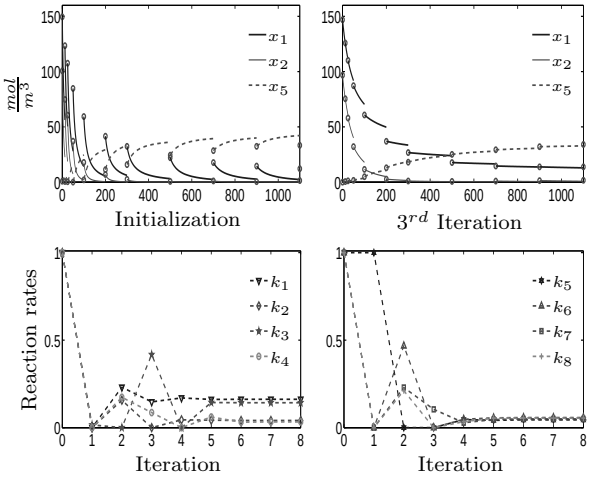


(a) Arbitrary initialization

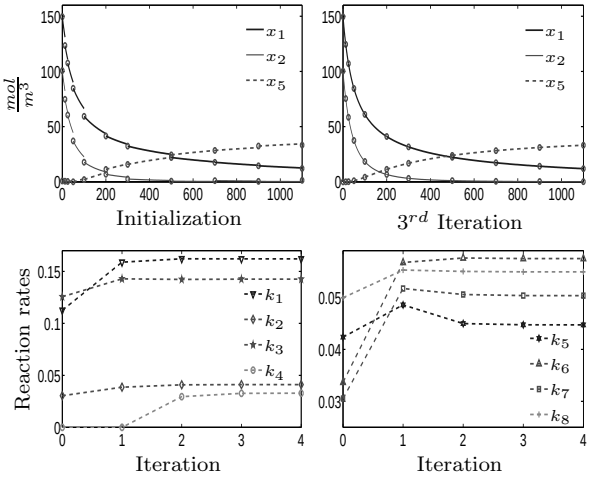


(b) Convex approach

Figure 13:

**Figure captions**

Figure 1: Homotopy map for the parameter estimation problem of a parameter-affine model. The original PEP is nonconvex ($\lambda \to 1$) but if the measured state sequence is used as the real state, it is possible to achieve convexity in one of the extremes of the map ($\lambda \to 0$). Notice that the presented approach only uses the convex extreme of the map and does not require continuity on the zero path.

Figure 2: Cost functions generated by the PEP of a harmonic oscillator when a noisy state sequence is measured (Top). NL corresponds to the original problem formulation while CVX to the convex approach. The plot in the bottom illustrates that the errors in the solution provided by the proposed approach are of second order in the size of the perturbation.

Figure 3: Multiple shooting approach. Parameters are represented by the local variables $p_i$ on each shooting interval and constrained to be equal to each other, i.e., $p_i = p_0$ for all $i = 1, 2, \ldots, N-1$.

Figure 4: Sparsity patterns for the Jacobians in a multiple shooting parameterization. In this example, the non-zero entries of the cost residuals Jacobian, and the equality and inequality constraints Jacobians are illustrated. The PEP involves four measurement points, $\bar{x}(t_i)$, $i = 0, 1, 2, 3$, two states, $x_1$, $x_2$, three parameters, $p_1$, $p_2$, $p_3$ and bound constraints on the parameters to estimate, $p^{\max}$ and $p^{\min}$.

Figure 5: Time evolution of the catalytic cracking of gas oil to gasoline. The noisy state measurements are taken from the benchmark problem for PE presented in Floudas et al. (1999).

Figure 6: Sum of Square Errors (SSE) for the parameter estimation problem of the catalytic cracking of gas oil. The state initial condition and parameter $k_3$ are fixed to $[1,\ 0]^T$ and 2, respectively.

Figure 7: Convergence results for the PEP of reaction rates in the catalytic cracking of gas oil. The PEP is parameterized using DMS and initialized arbitrarily and using the convex approach.

Figure 8: Set of noisy measurements used for the parameter estimation problem of the Lotka-Volterra model. Data has been generated by simulating the model with nominal parameters $p = [0.6,\ 0.5,\ 0.7,\ 0.4]^T$, $x(0) = [1,\ 0.5]$ and adding Gaussian noise with a variance $\sigma^2 = 0.05$.

Figure 9: SSE as a function of the variation of parameters $\alpha$ and $\gamma$ for the PEP in the Lotka-Volterra model. The parameters $\beta$, $\delta$ and the initial condition are constant and equal to their original values, i.e., $\beta = 0.5,\ \delta = 0.4,\ [x_1(t_0), x_2(t_0)]^T = [1, 0.5]^T$.

Figure 10: Convergence results for the simultaneous Gauss-Newton method applied to the PEP in the Lotka-Volterra model. The optimization is performed using and arbitrary initialization and the proposed convex approach.

Figure 11: Noisy states trajectories for the formaldehyde - sodium p-phenol sulfonate reaction. The dynamics is contaminated with Gaussian noise with standard deviation $\sigma = 1 \times 10^{-3}$ for $x_1$, $x_2$, $x_3$ and $x_5$ and $\sigma = 2.23 \times 10^{-4}$ for $x_4$, $x_6$ and $x_7$.

Figure 12: SSE as a function of the variation of parameters $k_1$ and $k_3$ for the PEP of the formaldehyde and sodium p-phenol sulfonate. The remaining 6 parameters and the initial condition are fixed to their nominal values.

Figure 13: Convergence results using the simultaneous Gauss-Newton algorithm for the PEP of the reaction rates in the reaction of formaldehyde with sodium p-phenol sulfonate. The figure illustrates the time evolution for the state trajectory using an arbitrary initialization (a) and the convex approach (b) along with the parameters convergence.

Table 1: Optimization Parameters for the Catalytic cracking of gas oil PEP using arbitrary and convex initialization approaches.

| Parameter | Arbitrary | Convex |
|---|---|---|
| $\mathrm{TOL}_{\mathrm{SQP}}$ | $1 \times 10^{-10}$ | $1 \times 10^{-10}$ |
| $\mathrm{ATOL}_{\mathrm{ODE}}$ | $1 \times 10^{-6}$ | $1 \times 10^{-6}$ |
| $\mathrm{RTOL}_{\mathrm{ODE}}$ | $[1,\ 1]\times 10^{-4}$ | $[1,\ 1]\times 10^{-4}$ |
| $\mathrm{KKT}_{\mathrm{TOL}}(p^*)$ | $4.253 \times 10^{-12}$ | $8.403 \times 10^{-11}$ |
| $\mathcal{J}(p^*)$ | $1.32766 \times 10^{-3}$ | $1.32766 \times 10^{-3}$ |
| $\mathrm{N}_{\mathrm{Iter}}$ | 4 | 3 |

Table 2: Algorithm parameters for the Lotka-Volterra PEP using arbitrary and convex initialization approaches.

| Parameter | Arbitrary | Convex |
|---|---|---|
| $\mathrm{TOL}_{\mathrm{SQP}}$ | $1 \times 10^{-10}$ | $1 \times 10^{-10}$ |
| $\mathrm{ATOL}_{\mathrm{ODE}}$ | $1 \times 10^{-6}$ | $1 \times 10^{-6}$ |
| $\mathrm{RTOL}_{\mathrm{ODE}}$ | $[1,\ 1]\times 10^{-4}$ | $[1,1\ ]\times 10^{-3}$ |
| $\mathrm{KKT}_{\mathrm{TOL}}(p^*)$ | $5.8486 \times 10^{-11}$ | $3.7386 \times 10^{-11}$ |
| $\mathcal{J}(p^*)$ | 0.80318 | 0.80318 |
| $\mathrm{N}_{\mathrm{Iter}}$ | 11 | 6 |

Table 3: Reaction rates for the batch reaction of formaldehyde with sodium p-phenol sulfonate.

| Reaction | Rate coefficient | Nominal value ($m^3$/kmol s) |
|---|---|---|
| A+B→C | $k_1$ | 0.16 |
| A+C→D | $k_2$ | 0.05 |
| C+D→E | $k_3$ | 0.15 |
| B+D→F | $k_4$ | 0.14 |
| C+C→F | $k_5$ | 0.03 |
| C+B→G | $k_6$ | 0.058 |
| A+G→F | $k_7$ | 0.05 |
| A+F→E | $k_8$ | 0.05 |

Table 4: Algorithm parameters for the complex batch reaction PEP using arbitrary and convex initialization approaches.

| Parameter | Arbitrary | Convex |
|---|---|---|
| $\mathrm{TOL_{SQP}}$ | $1 \times 10^{-10}$ | $1 \times 10^{-10}$ |
| $\mathrm{ATOL_{ODE}}$ | $1 \times 10^{-6}$ | $1{\times}10^{-6}$ |
| $\mathrm{RTOL_{ODE}}$ | $[1, 1]{\times}10^{-4}$ | $[1,1\ ]{\times}10^{-4}$ |
| $\mathrm{KKT_{TOL}}(p^*)$ | $9.8354 \times 10^{-11}$ | $1.556 \times 10^{-11}$ |
| $\mathcal{J}(p^*)$ | $1.6996 \times 10^{-5}$ | $1.6996 \times 10^{-5}$ |
| $\mathrm{N_{Iter}}$ | 8 | 4 |